# Resolution of Crossing Fibers with Constrained Compressed Sensing using Traditional Diffusion Tensor MRI

Bennett A. Landman[*a,d], Hanlin Wan[a,b], John A. Bogovic[b], Pierre-Louis Bazin[c], Jerry L. Prince[a,b,c]
[a]Biomedical Engineering, [b]Electrical and Computer Engineering, [c]Radiology,
Johns Hopkins University, Baltimore, MD, USA 21218
[d]Electrical Engineering, Vanderbilt University, Nashville, TN, USA 37235

## ABSTRACT

Diffusion tensor imaging (DTI) is widely used to characterize tissue micro-architecture and brain connectivity. Yet DTI suffers serious limitations in regions of crossing fibers because traditional tensor techniques cannot represent multiple, independent intra-voxel orientations. Compressed sensing has been proposed to resolve crossing fibers using a tensor mixture model (e.g., Crossing Fiber Angular Resolution of Intra-voxel structure, CFARI). Although similar in spirit to deconvolution approaches, CFARI uses sparsity to stabilize estimation with limited data rather than spatial consistency or limited model order. Here, we extend the CFARI approach to resolve crossing fibers through a strictly positive, parsimonious mixture model. Together with an optimized preconditioned conjugate gradient solver, estimation error and computational burden are greatly reduced over the initial presentation. Reliable estimates of intra-voxel orientations are demonstrated in simulation and *in vivo* using data representative of typical, low b-value (30 directions, 700 s/mm$^2$) clinical DTI protocols. These sequences are achievable in 5 minutes at 3 T, and the whole brain CFARI analysis is tractable for routine analysis. With these improvements, CFARI provides a robust framework for identifying intra-voxel structure with conventional DTI protocols and shows great promise in helping to resolve the crossing fiber problem in current clinical imaging studies.

**Keywords:** Diffusion weighted imaging, DTI, compressed sensing, crossing fibers

## 1. INTRODUCTION

Diffusion tensor imaging (DTI) provides non-invasive contrasts which are sensitive to *in vivo* cellular organization as modeled by local diffusivity, anisotropy, and tissue orientation [1-3]. The tensor model represents one independent, dominant direction, so that in voxels with complex fiber structure, the estimated orientation may be ambiguous or misleading [4]. Substantial efforts have been made to address this "crossing fiber" problem. One fruitful approach has been to acquire more detailed information through additional sensitized scans (e.g., diffusion spectrum [5], high angular resolution [6], q-ball [7], and high b-value [8] imaging techniques). Yet, scan time and hardware constraints limit widespread adoption of these methods in clinical research. Here, we seek to characterize regions of crossing fibers tissue using data acquired in conventional (i.e., low b-value, low angular resolution) DTI protocols.

Recently, there have been several indications that it is possible to resolve crossing-fibers from conventional DTI acquisitions provided that sufficient *a priori* information is available. Independent component analysis can exploit spatial information to fit a prolate tensor mixture [9], while cylindrically constrained two-tensor models have been numerically amenable to fitting using regularization techniques [10, 11]. Direct deconvolution with a discrete tensor basis set has also been used [12]. As these approaches are highly sensitive to noise, authors typically suggest limiting application to areas of known fiber crossing (e.g., planar tensor estimates) to avoid erroneous detections. Although initially developed as an alternative to Nyquist sampling, compressed sensing [13] offers a simple and elegant solution to the problem of regularized fitting of tensor models which does not require explicit model selection. Compressed sensing is on variant of many popular regularized regression methods (often referred to as LASSO techniques) [14, 15]. The recently presented Crossing Fiber Angular Resolution of Intra-voxel structure (CFARI) method uses this technique to reproducibly extract multiple fiber orientations per voxel [16].

* bennett.landman@vanderbilt.edu; http://iacl.ece.jhu.edu; Image Analysis and Communications Laboratory, Department of Biomedical Engineering, Johns Hopkins University, Baltimore, MD, USA 21218

Medical Imaging 2010: Image Processing, edited by Benoit M. Dawant, David R. Haynor,
Proc. of SPIE Vol. 7623, 76231H · © 2010 SPIE · CCC code: 1605-7422/10/$18 · doi: 10.1117/12.844171

In this manuscript, we extend the CFARI approach to fit a strictly positive mixture of tensor basis functions and reduce the computational burden through an optimized a preconditioned gradient solver. Accuracy at low SNR is improved, and consistent resolution of three fibers is demonstrated in simulation and *in vivo*. With CFARI, one can conduct whole brain analyses on a single CPU in less than 3 hours. Both the original and improved CFARI methods are implemented in the JIST (Java Image Science Toolkit) framework and are available in open source (http://www.nitrc.org/projects/jist/) [17]. With these improvements, CFARI provides a robust framework for identifying intra-voxel structure with traditional DTI and shows great promise in resolving the crossing fiber problem.

## 2. METHODS

CFARI models each voxel as a discontinuous collection of tissue compartments, which follow the traditional tensor model (Figure 1). Each voxel is parameterized as a finite mixture of discrete and independent compartments, and the diffusivity within each compartment is defined by the Stejskal-Tanner tensor formulation [18]. The observed signal, $S_k$, along the $k^{\text{th}}$ diffusion weighting direction ($\boldsymbol{g}_k$) is determined by the exponential mixture model,

$$S_k = S_0 \sum_i^N f_i e^{-b\ \boldsymbol{g}_k^T \mathbf{D}_i \boldsymbol{g}_k} + \eta. \tag{1}$$

$S_0$ is a noise-free reference signal in the absence of diffusion weighting, $N$ is the number of possible compartments (tensors) within each voxel, $f_i$ is the (unknown) mixture component for each compartment, $b$ is the diffusion sensitization parameter, $\mathbf{D}_i$ is the tensor associated with the $i^{\text{th}}$ compartment, and $\eta$ is a noise term that follows a Rician distribution. It is assumed that the *reconstruction basis* $\{\mathbf{D}_i\}$ — i.e., the set of possible diffusion tensors that may comprise a voxel — is fixed and known. Given this framework, the vector, $\boldsymbol{y}$, of $K$ observed attenuations, where each attenuation is defined as $y_k = S_k/S_0$, can be rewritten in matrix form as,

$$\boldsymbol{y}_{K\times 1} = \mathbf{S}_{K\times N}\boldsymbol{f}_{N\times 1} + \tilde{\boldsymbol{\eta}}_{K\times 1}, \tag{2}$$

where the matrix $\mathbf{S}$ comprises a set of exponential terms derived from Eq. (1) and $\tilde{\boldsymbol{\eta}}$ is a scaled noise term. In this model, The signal-to-noise (SNR) was defined as the ratio of the noise standard deviation on the complex coefficients and the (noise-free) unweighted signal intensity. At an SNR of greater than 5:1, Rician noise is well approximated by a Gaussian distribution, so a least squares estimator is appropriate [19]. With Eq.(2), we may immediately write the compressed sensing criteria,

$$\boldsymbol{f} = \text{argmin}_{\boldsymbol{f}:\boldsymbol{f}_i\in[0,\infty)} \|\mathbf{S}\,\boldsymbol{f} - \boldsymbol{y}\|_{L2} + \beta\|\boldsymbol{f}\|_{L1}, \tag{3}$$

where $\beta$ is a strictly positive *sparsity regularization parameter*. Note that the positivity restriction on $f_i$ is newly explored in this manuscript. Low $\beta$'s lead to least squares fitting of the observed signal with the specified basis, while high $\beta$'s force greater emphasis on a sparse model. There are efficient numerical methods to address optimization problems of the form of Eq. (3); in this work, we use the interior point method of Kim et al. [20] which includes the ability to enforce positivity constraints.

## 3. DATA

### 3.1 Simulations

The CFARI formulation is not dependent on the specific form of the diffusion weighted data to be analyzed. Here, we presume that we are interested in using either existing or conventional clinical research DTI data. Hence, the sensing basis — i.e., the choices of $b$-values and diffusion encoding directions — is considered to be determined by external requirements (such as reliability of clinical contrasts). There are two remaining design choices that must be addressed: the reconstruction basis and the sparsity regularization parameter.

In accordance with previous findings [16], the reconstruction basis $\mathbf{D}_i$'s are chosen to be cylindrically symmetric, of equal diffusivities, and regularly distributed on a sphere (fractional anisotropy of 0.71, principle eigenvalue of $2 \times 10^{-3}$ mm$^2$/s, 241 symmetric orientations) while the regularization parameter $\beta$ was selected to be 1.0 through empirical simulations to produce a tradeoff between minimal error and robustness against model mismatch. Monte Carlo

simulations were performed using two repetitions of 30 diffusion weighting directions (the "Jones30", [21]), $b$-value of 700 s/mm$^2$, five averaged unweighted reference acquisitions, and Rician distributed noise.

For all simulations, error was assessed as the mean angular difference between each estimated orientation and the closest orientation in the truth model, weighted by the estimated fraction:

$$E = \sum_i f_i \min_{j \in model} \angle(v_i, v_j). \quad (4)$$

The first simulation explored the effect of SNR on multiple tensor crossings. A single voxel was modeled with 1, 2, or 3 compartments. Each compartment had its directions chosen independently and uniformly at random from the reconstruction basis set. One thousand Monte Carlo iterations were employed to evaluate the error in CFARI estimation direction for each of 19 linearly spaced values of SNR from 5:1 to 50:1 (in steps of 2.5:1).

The second experiment compared unconstrained CFARI with the constrained CFARI. Again, a single voxel was modeled with 1, 2, or 3 compartments. Each compartment had its directions chosen independently and uniformly at random from the reconstruction basis set. One thousand Monte Carlo iterations were employed to evaluate the error in CFARI estimation direction for each of 19 linearly spaced values of SNR from 5:1 to 50:1 (in steps of 2.5:1).

Third, the effects of angular separation were explored in a simulated voxel with two compartments. Two tensors were generated at angles of 10º to 90º apart in 10º intervals. For each angle, the first tensor was randomly selected from the basis set. The second tensor was then chosen randomly from all the directions that were within 2º of the specified angle. An SNR of 25:1 was used.

Finally, a two-dimensional, three-crossing fiber model was simulated. Three tensors were selected to cross at 60º in plane. A 32 x 32 field of voxels was simulated with each fiber crossing at the center. The group membership was determined by having the compartment fraction fall off in a Gaussian manner from the center of each fiber. In regions of overlap, the centers of the fibers' compartment fractions were weighted equally. In regions without overlap of the central fibers, compartment fraction was assigned to the primary fiber and the "background." Note that a fourth, background component was added to the simulation (but not the basis set) with an isotropic component ($\lambda_1$=$\lambda_2$=$\lambda_3$=3x10$^{-3}$ mm$^2$/s). This forth compartment was not included in the reconstruction basis. Simulations were performed at SNR's of 10:1, 25:1, and 40:1.

### 3.2 In Vivo Experiment

A healthy volunteer with no history of neurological conditions was recruited. Local institutional review board approval and written informed consent were obtained prior to examination. All data were acquired using a 3T MR scanner (Achieva, Philips Medical Systems, Best, The Netherlands) with body coil excitation and an eight channel phased array SENSitivity Encoding (SENSE [22]) head-coil for reception. A DTI dataset was acquired with a multi-slice, single-shot, echo-planar imaging (EPI), spin echo sequence (TR/TE = 6281/67ms, SENSE factor = 2.5). Sixty-five transverse slices were acquired parallel to the line connecting the anterior commissure-posterior commissure (AC-PC) with no slice gap and 2.2 mm nominal isotropic resolution (FOV = 212 x 212, data matrix = 96 x 96, reconstructed to 256 x 256). Fat suppression as performed with Spectral Presaturation with Inversion Recovery (SPIR) and the phase encoding direction was anterior-posterior. Diffusion weighting was applied along 30 directions (Jones30; other parameters: gradient overplus = no, gradient mode = enhanced) with a b-value of 700 s/mm$^2$. The amplitude, leading edge spacing, and duration of the magnetic field gradients were G = 49 mT/m, $\Delta$ = 32.3ms, and $\delta$ = 12ms, respectively). The diffusion time, tdif, was 28.3ms (tdif = $\Delta$-$\delta$/3). Five minimally weighted images (5 b0's) (b ≈ 33s/mm$^2$) were acquired and averaged on the scanner as part of each DTI dataset. The total scan time to acquire the DTI dataset was 4 min 11s. No cardiac or respiratory gating was employed.

*In vivo* data were analyzed with CATNAP (http://iacl.ece.jhu.edu/~bennett/catnap/) [23]. Each diffusion weighted volume was registered to the unweighted reference volume. Diffusion weighting directions were corrected for relative rotations. Subsequently, CFARI was used to fit a multi-tensor model to each voxel in the acquired data. The basis set tensors were cylindrically symmetric, of equal diffusivities, and regularly distributed on a sphere (241 symmetric orientations distributed via potential energy minimization). Each basis tensor had a fractional anisotropy of 0.71 and principle eigenvalue of $2 \times 10^{-3}$ mm$^2$/s. The regularization parameter $\beta$ was one. The results were visually inspected for anatomical consistency. The boundary between the corpus callosum and the internal capsule was highlighted as a particularly relevant area of crossing fibers.

# 4. RESULTS

## 4.1 SNR Simulations

For all simulation models (e.g., 1, 2, or 3 tensors), increasing SNR resulted in decreasing estimation error across a wide range of SNR (Figure 2A). For one tensor, estimation error was less than 1º by 35:1 SNR (which is at the high end of clinical imaging). The error for a two tensor and three tensor model was higher (approximately 5º and 10º, respectively). At the lower end of SNR for clinical research DTI studies (15:1) all models had less than 15º error.

The positivity constraint on the CFARI estimator improved the error for experiments at less than 45:1 SNR (Figure 2B). The benefits of the positivity constraint were concentrated for the single compartment models. However, improvements of several percent were seen for both two compartment models and three compartment models at high SNR.

The mean error in constrained CFARI estimation was less than 10º error across the range of possible separations (see Fig 2C). Although the error was maximal (numerically) near 30º, the separation to noise ratio was greatest at the higher angular separations, so these separate fiber populations could be more robustly identified.

The in-plane crossing fibers could be visually resolved when three tracts cross with a separation of 60º in a plane (Figure 3). When a single fiber was mixed with a compartment with isotropic diffusivity (outside the indicated regions of interest), the primary orientation of the fiber is apparent at all three SNR's. In the central region (enlarged), the visual coherence of the three separate fiber bundles increases with increasing SNR. This result is consistent with the estimated error from the single voxel simulations.

## 4.2 In Vivo Results

White matter fibers running lateral through the corpus callosum and superior through the internal capsule are visible as coherent bundles on a coronal slice (Figure 4). In the region of their crossing, the primary path of the internal capsule (from inferior regions to motor cortex) is apparent. Additionally, the left-right course of the corpus callosum fibers is simultaneously apparent. On traditional tensor analyses, this region manifests as a "black hole." With CFARI, the pattern of crossing fibers is clearly identified regions and the results are consistent with anatomical expectations.

## 4.3 Simulation Time

Mean analysis time for constrained CFARI was 62 ms per brain voxel compared with 77 ms for unconstrained CFARI on a 1.6 GHz notebook computer.

# 5. CONCLUSION

CFARI provides a robust framework for identifying intra-voxel structure with conventional diffusion-weighted acquisitions and shows great promise in helping to resolve the crossing fiber problem. Although similar in spirit to existing deconvolution approaches, CFARI uses sparsity to stabilize estimation with limited data (rather than spatial consistency or a limited model order). As the current estimation process is driven only by information from individual voxels, one could exploit spatial regularization either in the subsequent fiber tracking or through direct incorporation of smoothing.

The single voxel experiments demonstrate that the angular resolution of the multiple compartment models is comparable to previously reported findings for q-ball peak detection and deconvolution based approaches (e.g., 10-20 degrees precision). The multiple intravoxel directions could be immediately used for probabilistic or deterministic fiber tracking in place of multi-orientation structures inferred by other methods. Calculation of generalized contrast measures, such as generalized fractional anisotropy (GFA) [7], is also straight forward.

The multi-compartment framework hints at other possibilities for characterizing tissue characteristics. It might be possible to associate specific basis component coefficient with different biophysical basis (e.g., types of tissue). Currently, the CFARI basis components vary only by orientation. In previous work, we saw that within this framework CFARI is robust to model mismatch. Lowering the FA of the basis set to improve robustness increases overall error. The CFARI numerical estimation framework readily supports non-tensor model for individual compartments. It would be fascinating to use either simulated or empirical observations of biological compartments of interests as a basis set. The utility of such an approach is, as yet, unproven and will be an exciting area of future research.

In summary, the simulations demonstrate that the positivity constraints in CFARI lead to stable and precise estimates of multiple intra-voxel compartmental directions. For the majority of models and SNR's explored, the additional constraint improved error over the unconstrained estimates and lead to more computational efficient estimates.

## ACKNOWLEDGEMENTS

We are grateful to Fatma El Zahraa ElShahaby for her assistance in improving this manuscript. This project was supported by NIH/NINDS 1R01NS056307, NIH/NIA N01-AG-4-0012, and NIH/NIDA 1K25DA025356.

*This work described herein has not been submitted elsewhere for publication or presentation.*

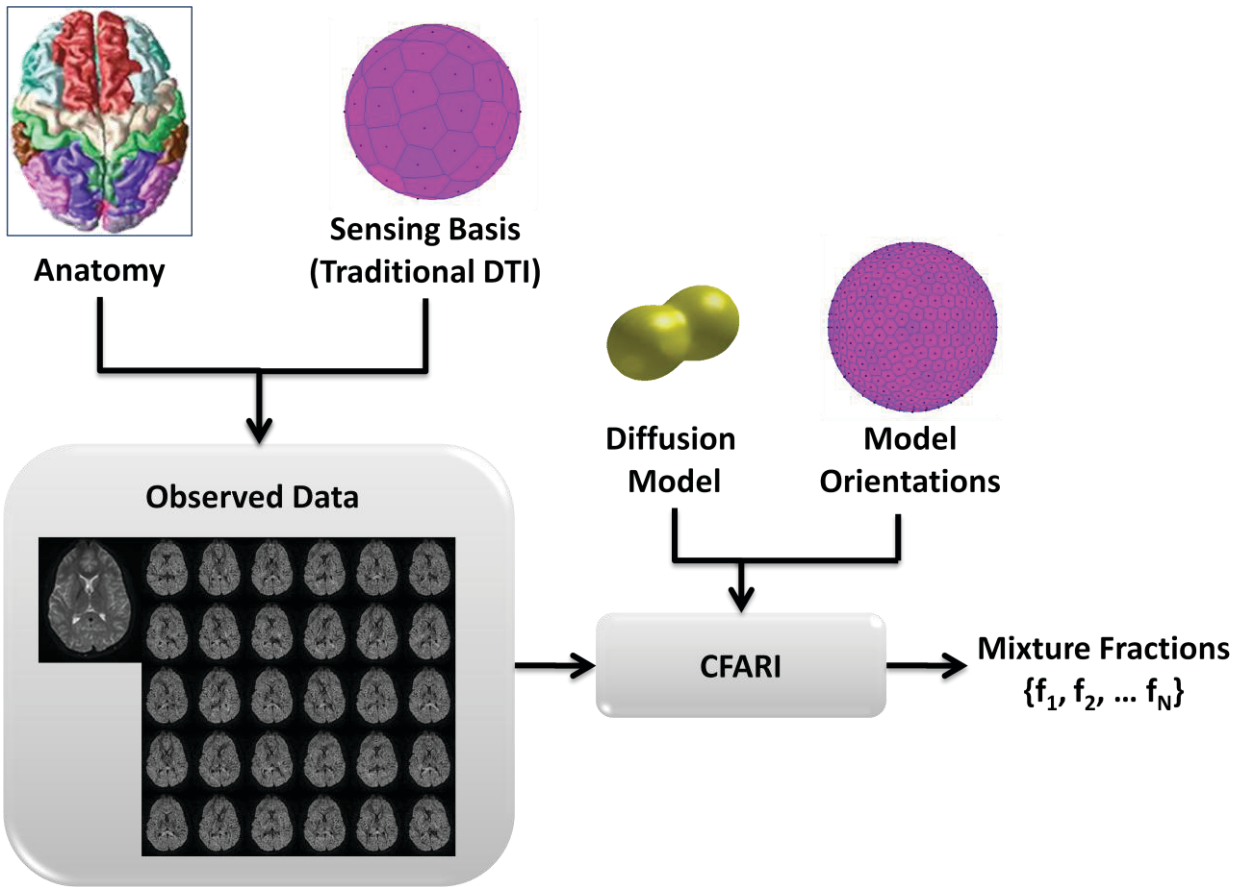


Figure 1. Overview of the CFARI Method. A traditional DTI acquisition is used to acquire data. For analysis, a mixture model consisting of a tensor model oriented along a large number of directions is fit to the observed data using a regularized regression approach.

## REFERENCES


[1] D. Le Bihan, and P. C. van Zijl, "From the diffusion coefficient to the diffusion tensor," NMR Biomed, 15(7-8), 431-434 (2002).

[2] P. J. Basser, and D. K. Jones, "Diffusion-tensor MRI: theory, experimental design and data analysis - a technical review," NMR Biomed, 15(7-8), 456-67 (2002).

[3] D. Le Bihan, J. F. Mangin, C. Poupon, C. A. Clark, S. Pappata, N. Molko, and H. Chabriat, "Diffusion tensor imaging: concepts and applications," J Magn Reson Imaging, 13(4), 534-46 (2001).

[4] M. R. Wiegell, H. B. Larsson, and V. J. Wedeen, "Fiber crossing in human brain depicted with diffusion tensor MR imaging," Radiology, 217(3), 897-903 (2000).

[5] V. J. Wedeen, T. G. Reese, D. S. Tuch, M. R. Weigel, J.-G. Dou, R. M. Weiskoff, and D. Chessler, "Mapping fiber orientation spectra in cerebral white matter with Fourier-transform diffusion MRI."

[6] L. R. Frank, "Characterization of anisotropy in high angular resolution diffusion-weighted MRI," Magn Reson Med, 47(6), 1083-1099 (2002).

[7] D. S. Tuch, "Q-ball imaging," Magn Reson Med, 52(6), 1358-72 (2004).

[8] J. D. Tournier, F. Calamante, D. G. Gadian, and A. Connelly, "Direct estimation of the fiber orientation density function from diffusion-weighted MRI data using spherical deconvolution," Neuroimage, 23(3), 1176-85 (2004).

[9] S. Kim, G. Chi-Fishman, A. S. Barnett, and C. Pierpaoli, "Dependence on diffusion time of apparent diffusion tensor of ex vivo calf tongue and heart," Magn Reson Med, 54(6), 1387-1396 (2005).

[10] S. Peled, O. Friman, F. Jolesz, and C.-F. Westin, "Geometrically constrained two-tensor model for crossing tracts in DWI," Magn Reson Imag, 24(9), 1263-1270 (2006).

[11] N. S. Stamatios, B. Li, S. M. Paul, P. A. Dorothee, S. C. Cris, and R. T. Christopher, "A regularized two-tensor model fit to low angular resolution diffusion images using basis directions," Journal of Magnetic Resonance Imaging, 28(1), 199-209 (2008).

[12] A. Ramirez-Manzanares, M. Rivera, B. C. Vemuri, P. Carney, and T. Mareci, "Diffusion basis functions decomposition for estimating white matter intravoxel fiber geometry," IEEE Trans Med Imaging, 26(8), 1091-102 (2007).

[13] M. Lustig, D. L. Donoho, J. M. Santos, and J. M. Pauly, "Compressed Sensing MRI [A look at how CS can improve on current imaging techniques]," IEEE Signal Processing Magazine, 25(2), 72 - 82 (2008).

[14] B. Efron, I. Johnstone, T. Hastie, and R. Tibshirani, "Least angle regression " Annals of Statistics 32(2), 407–499 (2003).

[15] R. Tibshirani, "Regression shrinkage and selection via the lasso," J. Royal. Statist. Soc B., 58(1), 267-288 (1996).

[16] B. A. Landman, J. Bogovic, and J. L. Prince, [Compressed Sensing of Multiple Intra-Voxel Orientations with Traditional DTI], New York, NY(2008).

[17] B. C. Lucas, J. A. Bogovic, A. Carass, P.-L. Bazin, J. L. Prince, D. Pham, and B. A. Landman, "The Java Image Science Toolkit (JIST) for Rapid Prototyping and Publishing of Neuroimaging Software," Neuroinformatics, (In press 2010).

[18] E. O. Stejskal, and J. E. Tanner, "Spin diffusion measurements: spin echoes in the presence of a time-dependent field gradient," J Phys Chem, 42, 288-292 (1965).

[19] H. Gudbjartsson, and S. Patz, "The Rician distribution of noisy MRI data," Magn Reson Med, 34(6), 910-4 (1995).

[20] S.-J. Kim, K. Koh, M. Lustig, S. Boyd, and D. Gorinevsky, "A method for large-scale l1-regularized least squares," IEEE Journal on Selected Topics in Signal Processing, 1(4), 606–617 (2007).

[21] S. Skare, M. Hedehus, M. E. Moseley, and T. Q. Li, "Condition number as a measure of noise performance of diffusion tensor data acquisition schemes with MRI," J Magn Reson, 147(2), 340-52 (2000).

[22] P. P. Klaas, W. Markus, B. S. Markus, and B. Peter, "SENSE: Sensitivity encoding for fast MRI," Magnetic Resonance in Medicine, 42(5), 952-962 (1999).

[23] B. A. Landman, J. A. Farrell, C. K. Jones, S. A. Smith, J. L. Prince, and S. Mori, "Effects of diffusion weighting schemes on the reproducibility of DTI-derived fractional anisotropy, mean diffusivity, and principal eigenvector measurements at 1.5T," Neuroimage, 36(4), 1123-38 (2007).

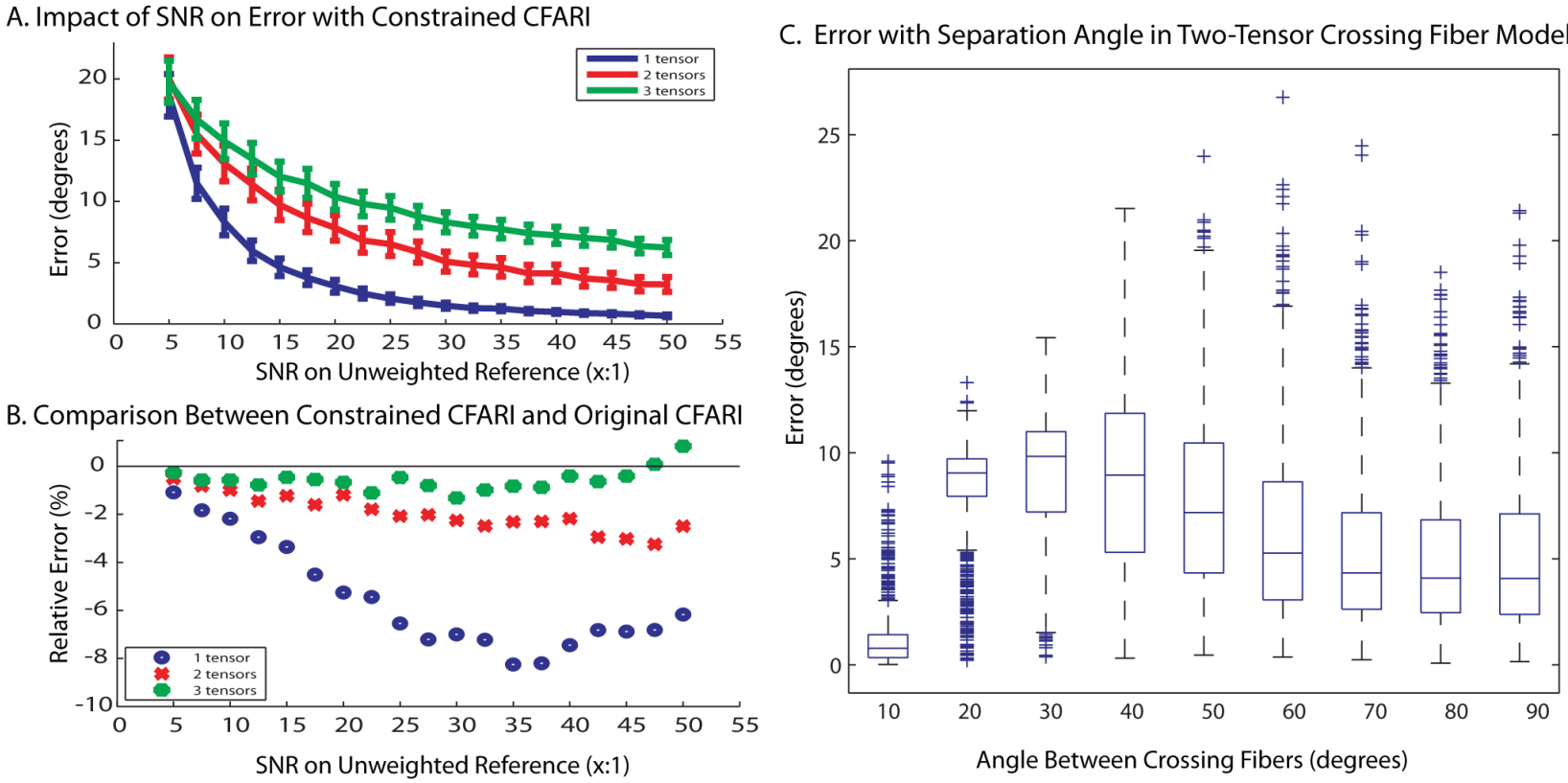


Figure 2. Impacts of SNR on CFARI intra-voxel direction estimation. Error increased with the presence of multiple true intra-voxel structures, but was within approximately 10º for an SNR of greater than 25:1 (A). The newly developed constrained CFARI approach resulted in lower error than the original approach at typical SNR (B). Median error for two-tensor models was less than 15º regardless of crossing angle (C).

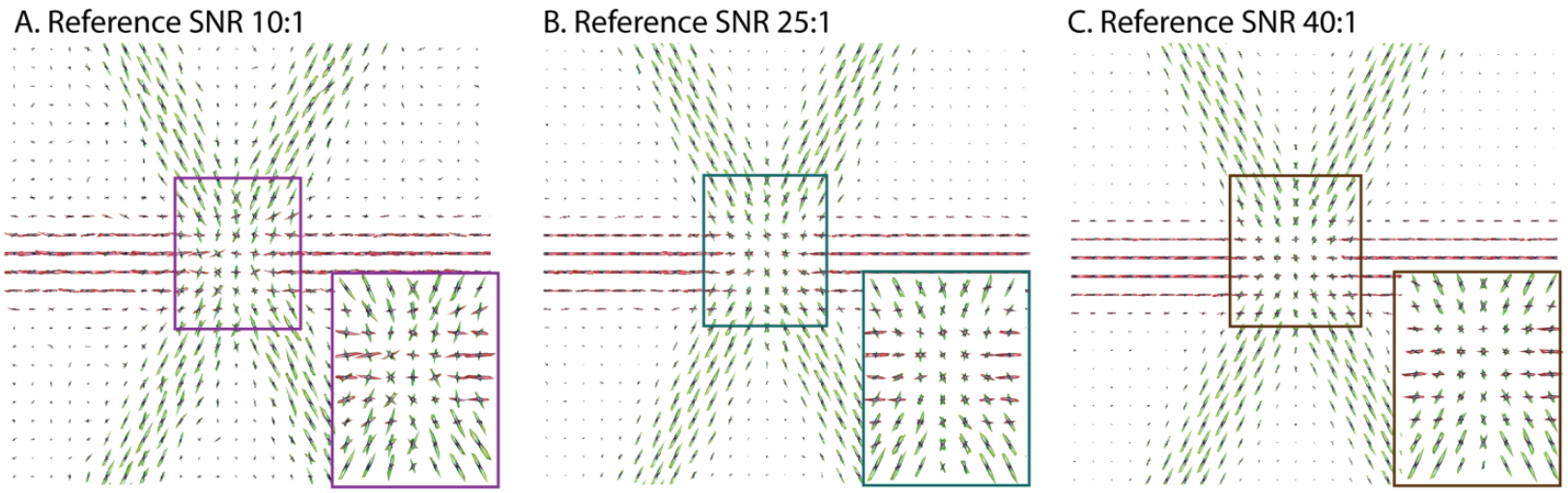


Figure 3. Increased SNR improves the consistency of estimated intra-voxel structure (compare A to B to C). However, three distinct crossing fibers are clearly apparent at a typical clinical SNR of 25:1.

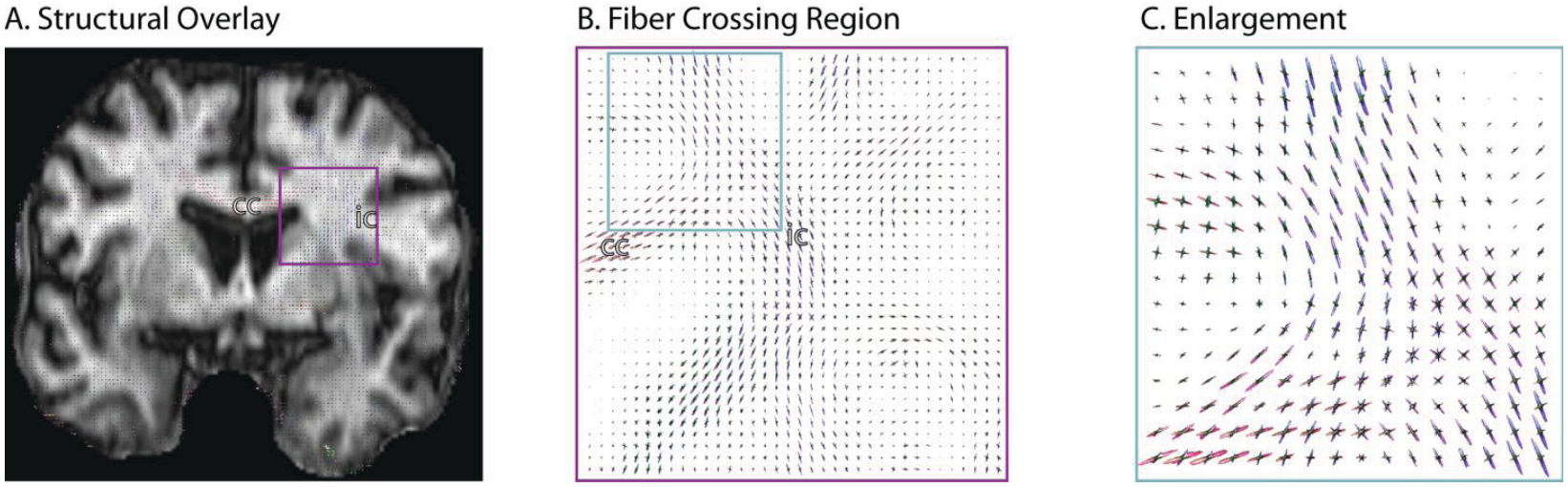


Figure 4. Intra-voxel orientations estimated with *in vivo* data show patterns consistent with anatomy, which can be clearly appreciated in the region of the corpus callosum (cc) and internal capsule (ic).